Effects of Titanium Dioxide and Zinc Oxide Nano-materials on Lipid Order in Model Membranes

Matthew J. Sydor[†,*], **Donald S. Anderson**[†], **Harmen B.B. Steele**[‡,§], **J.B. Alexander Ross**[‡,§], **Andrij Holian**[†]

[†]Center for Environmental Health Sciences, Department of Biomedical and Pharmaceutical Sciences, University of Montana, Missoula, MT 59812

[‡]Department of Chemistry and Biochemistry, University of Montana, Missoula, MT 59812

[§]Center for Biomolecular and Structure & Dynamics, University of Montana, Missoula, MT 59812

Abstract

Engineered Nano-materials (ENM) have been reported to affect lipid membrane permeability in cell models, but a mechanistic understanding of how these materials interact with biological membranes has not been described. To assess mechanisms of permeability, liposomes composed of DOPC, DOPS, or POPC, with or without cholesterol, were used as model membranes for measuring ENM-induced changes to lipid order to improve our understanding of ENM effects on membrane permeability. Liposomes were treated with either titanium dioxide (TiO_2) or zinc oxide (ZnO) ENM, and changes to lipid order were measured by time-resolved fluorescence anisotropy of a lipophilic probe, Di-4-ANEPPDHQ. Both ENM increased lipid order in two lipid models differing in headgroup charge. TiO_2 increased lipid order of POPC liposomes (neutral charge), while ZnO acted primarily on DOPS liposomes (negative charge). Addition of cholesterol to these models significantly increased lipid order while in some cases attenuated ENM-induced changes to lipid order. To assess the ability of ENM to induce membrane permeability, liposomes composed of the above lipids were assayed for membrane permeability by calcein leakage in response to ENM. Both ENM caused a dose-dependent increase in permeability in all liposome models tested, and the addition of cholesterol to the liposome models neither blocked nor reduced calcein leakage. Together, these experiments show that ENM increased permeability of small molecules (calcein) from model liposomes, and that the magnitude of the effect of ENM on lipid order depended on ENM surface charge, lipid head group charge and the presence of cholesterol in the membrane.

Graphical Abstract

---

[*]**indicates corresponding author:** University of Montana, 32 Campus Drive, Missoula, MT, 59812, matthew.sydor@umontana.edu.

Declaration of competing interest

The authors declare that they have no known competing financial interests or personal relationships that could have appeared to influence the work reported in this paper.

Fluorscence Probe

ENM-induced Lipid Order
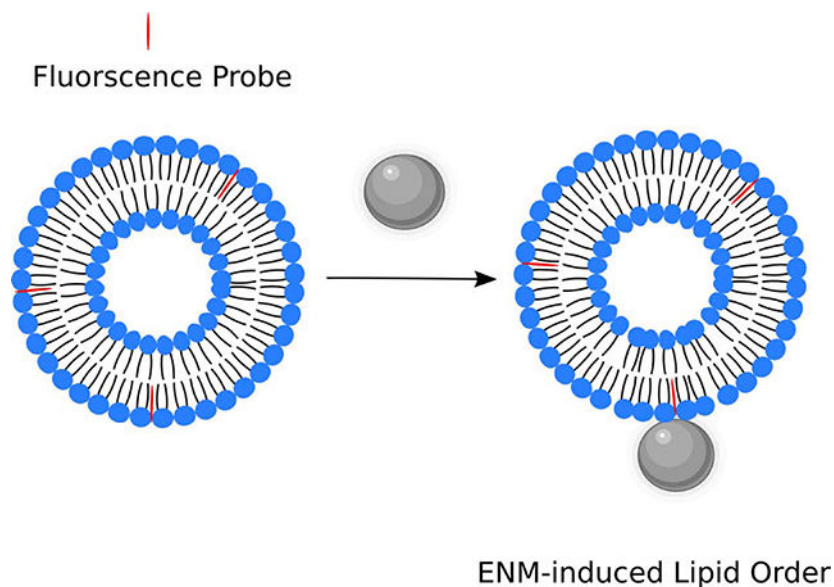
Keywords

Titanium Dioxide; Zinc Oxide; anisotropy; Liposome; Model Membrane

1.0   Introduction

Engineered nano-materials (ENM) encompass a wide variety of materials, the use of which is becoming more prevalent in today's consumer products, as well as in biomedical applications, such as therapeutics and diagnostics. According to the Project on Emerging Nanotechnologies, there are over 1800 consumer products that contain ENM[1]. With this increased use of ENM, the concern for human exposure to such materials has increased. Since human cells can come into contact with these materials, the interaction of such materials with biological lipid membranes must be understood. One of the major routes of ENM exposure is by inhalation[2,3]. After inhalation, immune cells, such as alveolar macrophages can phagocytose these materials, leading to their internalization[4–6]. Following phagocytosis by alveolar macrophages, the ENM are eventually encapsulated within phagolysosomes. We have reported, as well as others, that ENM can induce phagolysosomal membrane permeability (LMP) in cells, thereby causing the release of lysosomal degradative enzymes into the cytosol, inducing inflammation[7–18]. We have proposed that when ENM interact with lipid membranes, that a change to the order of the lipid membrane will occur, that will progress to an increase in phagolysosomal membrane permeability. In addition, it has been shown that changing cholesterol content in lysosomal membranes is a significant modifier of LMP [19,20].

Although, much is known about how ENM cause inflammation, little is known about what causes LMP to occur and what effects ENM have on lipid membranes, resulting in LMP. The ability to understand and prevent LMP would present new options for mitigating the adverse health effects of the ENM-induced inflammation. Also, a basic understanding of

ENM - lipid membrane interactions will be helpful in the design of not only safer to handle ENM and could lead to discovery of better targeted drugs and therapeutics. Therefore, in order to bridge this gap of knowledge, an improved understanding of how ENM affect lipid membranes is necessary. Here, ENM-lipid membrane interactions were studied by treating unilamellar liposomes of various phospholipid compositions (DOPC, POPC, and DOPS) with two common high volume ENM, titanium dioxide (TiO_2) or zinc oxide (ZnO), which are 24 and 20 nm in size, respectively. Titanium dioxide has a surface area of 53 m^2/g while the surface area of zinc oxide is 26 m^2/g. Both TiO_2 and ZnO are spheroid and have zeta potentials at pH 7.4 in tris-buffered saline of −7.81 ± 3.6 and −10.4 ± 4.5, respectively. These well characterized materials were selected because of their similarity in type (metal oxide), size, and their ability to be suspended and dispersed in aqueous buffers without the need of a surfactant but differ in surface charge at neutral pH, where TiO_2 has essentially zero charge and ZnO has a strong positive charge[21,22]. Both of these ENM have been reported to cause LMP *in vitro* with ZnO being more bioactive than TiO_2. At similar doses ZnO causes greater LMP than TiO_2 in macrophages[8,23]. In addition, we examined the contribution of cholesterol to membrane order and influence on the effects of the two ENM. In our work, both materials caused increased lipid order although with different lipids that were modified by cholesterol and both ENM increased permeability to calcein. We propose that these interactions between ENM and liposomes of lipid order/disorder of the membrane are important outcomes in cells.

2.0 Methods

2.1 Materials

The following lipids were purchased from Avanti Polar Lipids, Inc. (Alabaster, AL): 1-palmitoyl-2-oleoyl-glycero-3-phosphocholine (POPC) (Cat# 850475), 1,2-dioleoyl-sn-glycero-3-phosphocholine (DOPC) (Cat# 850375), 1,2-dioleoyl-sn-glycero-3-phospho-L-serine (sodium salt) (DOPS) (Cat# 840035), and cholesterol (ovine) (Cat# 700000). 1-[2-Hydroxy-3-(N,N-di-methyl-N-hydroxyethyl)ammoniopropyl]-4-[β-[2-(di-n-butylamino)-6-napthyl] vinyl]pyridinium dibromide (Di-4-ANEPPDHQ) (Cat# D36802) was purchased from ThermoFisher (Waltham, MA). Titanium dioxide P225 (81% anatase, 19% rutile) and zinc oxide were obtained from Evonik (Parsippany, NJ) and Meliorum Technologies Inc. (Rochester, NY), respectively.

2.2 Liposome Preparation

All phospholipids were purchased from Avanti Polar Lipids, Inc. as chloroform solutions. Cholesterol was dissolved in HPLC grade B&J Chloroform, containing amylene and 1% ethanol preservatives at 5 mg/ml. Appropriate concentrations were dried for at least one hour under a stream of nitrogen gas. The lipid films were then hydrated in a 50 mM tris (pH 7.4), 150 mM NaCl buffer (TBS). Lipids were then sonicated in a bath sonicator for 10 minutes with vortexing once every minute. Liposomes, either 100 or 400 nm in diameter, were generated using an Avanti Polar Lipids, Inc. mini extruder heated 10°C above the phase transition temperature of the lipid.

2.3   Time-resolved Anisotropy Decay Measurements

To perform time-resolved anisotropy measurements, 100 nm liposomes were used. For each sample, 0.85 mg of lipid was used to form liposomes as described above. ENM stock suspensions were prepared at 1 mg/ml in the buffer listed above and sonicated for 2 min in a Qsonica (Newtown, CT) Q500 sonicator. ENM were then mixed with the liposome suspension at the desired concentration and placed in a tube rotator at 37°C for 2 hours. Di-4-ANEPPDHQ was dissolved in spectral grade DMSO and added to the liposome samples at a concentration of 400 nM (final DMSO concentration of <1%). The dye was allowed to incubate at room temperature with the liposomes for 15 minutes before data acquisition, in order to simulate incorporation of the dye into cells[24,25]. Fluorescence measurements were collected using a custom-built fluorimeter (Quantum Northwest, Liberty Lake, WA) as previously described[26]. The probe, Di-4-ANEPPDHQ was excited by a 470 nm pulsed diode laser (LDH-P-C-470; PicoQuant, Berlin GmbH). Fluorescence emissions were isolated by a 500 nm longpass filter (Chroma, Bellows Falls, VT) and detected using an Edinburgh Instruments (Livingston, UK) photomultiplier tube (H10720–01). Measurements were taken at 18.5 ± 0.02°C. Anisotropy decay measurements were analyzed using FluoFit v4.6.6 (PicoQuant, Berlin GmbH).

2.4   Liposome Lysis Assay

Liposomes that were 400 nm in diameter were prepared as described above. In this assay, the hydration of the lipid film was performed with 50 mM calcein solution in TBS. The calcein (ThermoFisher, Waltham, MA Cat# C481) solution was made by mixing calcein powder in TBS with stirring, low heat, and adjusting the pH to 7.4 with NaOH. The liposomes were then vortexed and extruded with a 400 nm filter. Free calcein was separated from the liposomes by gel filtration of 1 ml liposome samples using a 10 ml column of Sepharose cl-4b (GE Life Sciences, Pittsburgh, PA) with TBS as the eluent. The eluted samples were diluted 16-fold in TBS and stored at 4°C for use within 48 hours. The appropriate amount of ENM was added to each tube, followed by incubation at 37°C with tumbling for 2 hours. All fluorescence intensity measurements were taken on a SpectraMax M4 (Molecular Devices, San Jose, CA) with excitation at 490 nm and emission at 520 nm. A background fluorescence measurement was taken immediately after particles were added. Another was taken after the 2-hour incubation, and finally a total fluorescence measurement was acquired after adding 10 μl of 1% Triton-x to each sample. The leakage of each sample was calculated as a percent by using equation #3, appendix. This procedure was based on the work of Alkhammash *et al.* (27). An example emission spectra of calcein-loaded liposomes is displayed in appendix Figure 1.

2.5   Statistical Analyses

Two-tailed, unpaired t-tests to compare two means, along with one-way ANOVA with Dunnett post-test, were performed using Statistica 176 (TIBCO Software, Inc.). P-values < 0.05 were determined to be statistically significant.

3. Results

To elucidate changes to the order of the model membranes, time-resolved fluorescence anisotropy measurements were utilized. Time-resolved anisotropy directly reports the rate of depolarization of the emission of fluorophores incorporated in lipid membranes where the degree of depolarization is a measure of the lipid order. In these studies, a lipophilic fluorescence probe, Di-4-ANEPPDHQ, was used to report changes in the lipid order of model membranes as a result of ENM-liposome interaction. Di-4-ANEPPDHQ is solvatochromic and incorporates into both the ordered and disordered phases of lipid membranes. Previous characterization work with this probe by our laboratory, and others, has demonstrated that its spectra and anisotropy are sensitive to the local environment in the membrane. Thus, Di-4-ANEPPDHQ is suitable for detecting changes to lipid order/disorder in cells and model systems[28–30].Time-resolved anisotropy parameters were determined by equation #1 (see appendix)[31]. Following acquisition, the data were analyzed using the wobble-in-a-cone model, equation #2, appendix. The cone-angle value, θ, can be used to describe the wobble and constraint of the fluorescence probe in the lipid bilayer[32,33].

Thus, θ indicates the lipid order around the probe, Di-4-ANEPPDHQ. The lipids selected for this study, shown in Table 1, were chosen based on the working hypothesis that if ENM disrupt lipid membranes, the composition of phospholipid headgroups and tail-groups will play a role in whether or not this disruption takes place and the extent of the effects. The phospholipids used in these studies had two types of headgroups: phosphatidylcholine (neutral zwitterion) or phosphatidylserine (negatively charged). The length and saturation of the acyl chains of the phospholipids were either 16:0–18:1 or 18:1. These lipids were chosen because both phosphatidylcholine and phosphatidylserine are biologically relevant and prevalent in the lysosomes of mammalian cells[35]. In this study, both approximately 100 nm and 400 nm sized liposomes were used. Average size data determined by DLS for liposome extruded through 100 nm and 400 nm filters was 128 ± 39 and 459 ± 49, respectively. Zeta potential measurements at pH 7.4 in tris-buffered saline were taken for POPC, DOPC, and DOPS, which were -1.1 ± 2, 0.1 ± 1.4, and -2.76 ± 1, respectively.

Cholesterol is one of the most abundant lipids in mammalian cells, and has been implicated in modifying the lipid order of the membrane for appropriate cellular function[33]. In particular, cholesterol has been observed to increase the favorable packing of the acyl chains in model phosphatidylcholine systems[34–36]. Therefore, we also examined how cholesterol affects (mitigates) the action of ENM on the model membranes. In order to demonstrate the impact of cholesterol on the model membranes in this study, cholesterol was incorporated into DOPC, DOPS, and POPC 100 nm liposomes. Figure 1 displays time-resolved anisotropy data for these liposomes, with or without cholesterol, at an equal mass ratio. In this way, two systems were generated with definitive differences in lipid order and cholesterol content for determining how the change in membrane properties affects ENM-induced disruption. The addition of cholesterol to all three model systems resulted in a significant reduction in the cone angle of the probe Di-4ANEPPDHQ with the largest change occurring in POPC liposomes. The data is consistent with the prediction that cholesterol can cause an increase in lipid order and packing in model membranes and cells[24,37].

To better understand how the phospholipid headgroups impact ENM-induced membrane disruption, DOPC, DOPS, and POPC 100 nm liposomes, with or without cholesterol, were treated with 100 μg/ml TiO$_2$ or ZnO for two hours prior to time-resolved anisotropy measurements.

To measure how changes to lipid order affect membrane permeability, an assay was employed that utilized the self-quenching properties of the small (MW 622.54) fluorescent molecule, calcein[27,38]. When released from permeabilized liposomes, dilution reverses the self-quenching and the fluorescence intensity increases. The assay involved loading 400 nm liposomes with 50 mM calcein solution and the excess calcein outside of the liposomes was removed by gel filtration; membrane permeability caused by ENM was expected to result in an increase in calcein fluorescence. The liposomes were diluted such that their total surface area was equal to the surface area of the 100 nm liposomes in the anisotropy experiments. Consequently, the liposome to ENM surface area ratio for both studies remained the same. The doses of ENM were 25 μg/ml and 100 μg/ml with 2-hour incubations at 37°C with gentle mixing. The amount of leakage was calculated as a percent, determined by equation #3, appendix. Lastly, to determine the effects of cholesterol on liposome leakage, DOPC, POPC, and DOPS 400 nm liposomes were prepared in an equal mass ratio of phospholipid to cholesterol, and the assay was performed as above.

Figure 2 displays anisotropy data in cone angle form and calcein leakage data for DOPC liposomes treated with TiO$_2$ or ZnO. Treatment with either particle did not produce a significant change in the cone angle displayed in Figure 2A, however, the high doses of TiO$_2$ and ZnO both caused increased calcein leakage compared to control levels, which is shown in Figure 2B. As shown in Figure 2C, TiO$_2$ caused a decrease to the cone angle of the DOPC-chol liposomes, while ZnO did not. The same liposomes showed an increase in leakage caused by the ENM, Figure 2D, however, the differences were not statistically significant. The p-values for the comparison between the high doses of TiO$_2$ and ZnO and the DOPC-chol control were 0.086 and 0.11, respectively.

The results of the DOPS membrane model are displayed in Figure 3. In contrast to its effect on DOPC, ZnO produced a significant decrease in the cone angle of DOPS liposomes (29.4%); TiO$_2$ did not alter the cone angle significantly, as shown in Figure 3A. These results indicate that the negative charge of the DOPS headgroup appears to have a role in the interaction of ZnO with DOPS and the resulting restriction of the membrane lipid mobility. DOPS leakage results shown in Figure 3B were similar to those of DOPC in that, again, the 100 μg/ml dose of both particles caused significant increases in the percent leakage. ZnO increased order in membranes containing DOPS. However, with the presence of cholesterol, Figure 3C, the amount by which the cone angle decreased was attenuated. Since the DOPS and cholesterol mixture is inherently more ordered, the order induced by the ZnO was less. Finally, as shown in Figure 3D, DOPS-chol liposomes were tested with both ENM, and there was significant leakage at 100 μg/ml TiO$_2$, as well as, at the 25 and 100 μg/ml doses of ZnO. Here it appears that ZnO has a greater effect than TiO$_2$ which is consistent with the known greater effects on LMP[4,8,39,40].

To determine if the length and saturation of the acyl chains on the lipids influenced the ENM-liposome interactions, POPC liposomes were exposed to both ENM. The results in Figure 4A demonstrate that TiO_2 caused a significant decrease in the cone angle of POPC liposomes, while ZnO did not have a significant effect. These data indicate that TiO_2 appears to interact with POPC, while ZnO acts on DOPS liposomes. Comparatively, TiO_2 did not have this effect on DOPC liposomes. This outcome may be explained by the double bond on both acyl chains of DOPC compared to POPC, which has one saturated acyl chain. Additionally, one acyl chain of POPC is slightly shorter than that of DOPC, possibly making it more easily susceptible to an increase in order caused by TiO_2. Similar to both DOPC and DOPS liposomes, the 100 µg/ml dose of both ENM caused significant increases in the calcein leakage from POPC liposomes, displayed in Figure 4B. The addition of cholesterol to this model attenuated the change in cone angle but not the increase in membrane permeability, as shown in Figure 4C and D. The mean cone angle of POPC with TiO_2 treatment decreased from 33.9° to 27.9° (Table appendix), while with the addition of cholesterol TiO_2 treatment produced a decrease from 16.7° to 13.9°.

4. Discussion

In this study, two different assays were used to determine the effects of ENM-induced lipid membrane disruption. Time-resolved anisotropy was used to determine changes in the lipid order of model liposome systems. Treatment with ENM resulted in decreased wobble-in-a-cone angle, representing increased lipid packing (increased order) around the probe, Di-4ANEPPDHQ. We propose that these changes are a result of ENM, when near or interacting with the phospholipid surface, restricting lipid motion. This restriction, may cause a disruption in other regions of the membrane away from the ENM, resulting in the calcein leakage. For example, an ENM interaction with a portion of the liposome would result in a localized increase in lipid order by restricting phospholipid motion. This phospholipid restriction in one region may allow more space between phospholipids in another region of the same liposome, resulting in leakage of calcein. Overall, the data demonstrate that both ENM have similar effects on the different model lipid membranes examined in this study. However, an important finding is that the two ENM appear to interact with different headgroups. Phosphatidylcholine lipids seem to be the most affected by TiO_2 with POPC and DOPC-chol cone angles being reduced, indicating increased localized order in the membrane. In contrast, ZnO caused a significant reduction in the cone angle of DOPS liposomes. Similar changes in anisotropy were caused by both ENM with the difference being which lipids were affected. These differences may be physiologically relevant since ZnO has been shown to cause more LMP and be more toxic to cells than TiO_2[23].

Addition of cholesterol caused a marked reduction in the baseline cone angle of the model systems, which is a result of cholesterol increasing lipid packing and thus increasing order. However, addition of cholesterol did not completely abolish ENM-induced membrane disruption. Cholesterol reduced the anisotropy change of both ZnO on DOPS-chol liposomes and TiO_2 on POPC-chol liposomes Nevertheless, the decrease caused by cholesterol may be physiologically relevant and explain the protective effects of increasing cholesterol in lysosomes by blocking LMP[19,20]. The addition of cholesterol by itself caused

a change to the lipid order of the system. This change, however, did not significantly block the ability of the ENM to induce calcein leakage. This may be due to the size of the calcein molecules, meaning that the increase in lipid order by cholesterol was not enough to block the diffusion of calcein out of the liposome. In macrophages, ENM have been reported to induce lysosomal membrane permeability with the diffusion of proteins out of the lysosome that cholesterol levels modulate[8,19,20]. Future work will be necessary to determine what size of molecules can leak out of ENM-disrupted membranes.

The calcein permeability assay was performed to measure ENM-induced lipid membrane permeability to small molecules. All three model systems, DOPC, DOPS, and POPC, demonstrated significant increases in calcein leakage in response to the high doses of ENM. These results appear to be in contrast to the anisotropy data, which were dependent both on lipid headgroup charge and ENM type. The anisotropy reporter probe is most likely distributed uniformly in unperturbed liposomes. However, interaction with ENM would be expected to affect the dynamics of those probes located in the vicinity of ENM, and observable anisotropy changes would require enough ENM to be interacting with the liposomes at one time in order to measurably shift the now non-uniform distribution of the probes in the liposomes. Comparatively, the calcein permeability assay appears to be more sensitive, as only a small disruption/pertubation is likely needed to cause leakage of calcein, which was easily detected by changes in fluorescence intensity. Moreover, the calcein leakage assay directly measured the ability of ENM to cause membrane permeability to the small molecule calcein, while the cone angle from the anisotropy measurements represents how ENM may be causing the membrane permeability. These two assays were used to measure different parts of the same effect. Among the calcein leakage results, there were differences in control leakage levels, depending on the type of lipid. The DOPC and POPC control levels were 33.2% and 28.1%, respectively and much higher than DOPS (7.8%). This is likely due to high permeability of the calcein through the DOPC and POPC liposomal membranes since it is a small molecule and the lipid headgroups have neutral charge. In comparison, DOPS baseline leakage levels were much lower probably because of charge repulsion between the negatively charged calcein (at pH 7.4) and the phosphatidylserine headgroup. It should be noted that ZnO caused a greater effect on calcein leakage in the DOPS model than TiO_2, which may be more physiologically relevant.

The changes in anisotropy clearly indicate that an interaction occurred between the ENM and liposome membrane. Our study used a different model and assessments than other studies which used computer simulations to study the interaction between metal nano-materials and lipid membranes. Cationic gold nanoparticles were reported to translocate through the lipid membrane with the opening of a pore facilitating the translocation[41]. In another study, bare nanoparticles were observed to directly interact with a lipid membrane, allowing for integration of the particle into the lipid bilayer, which was preventable by the addition of a protein corona[42]. Various other studies have been conducted with cells and report that nanoparticles can translocate through the plasma membrane and cause depolarization of the cell's membrane, possibly through a similar mechanism as in the computer modeling publications[43–45]. Other studies have reported that nanoparticles can adsorb to liposomes and cause membrane permeability to calcein molecules with adsorption being the step preceding leakage. Various factors such as charge, pH, and salt concentration

can affect these events[46,47]. Taken together, these reports further support the notion that bare ENM and lipid membranes can interact resulting in membrane disruption and permeability.

5.0 Conclusions

Previous studies have reported that ZnO is more bioactive and causes more LMP in macrophages than TiO_2[6,8,23,39]. This prompted our interest to develop the models and approaches to evaluate the mechanism of membrane disruption between two ENM of similar size, but with distinct differences in charge. Both ENM caused calcein leakage from liposomes composed of lipids with headgroups having either neutral or negative charge although the effects were different depending on lipids and ENM. Furthermore, the addition of cholesterol increased the order of the model systems and attenuated some ENM-induced membrane changes. However, cholesterol did not have a large-scale effect on the amount of calcein leakage due to ENM. A potential explanation is that calcein is a small molecule and the changes to lipid order caused by the cholesterol were not sufficient to inhibit movement of this small molecule across the lipid bilayer. Additional studies will be necessary to measure the ability of ENM to cause release of larger biomolecules, such as proteins of various sizes (viz., similar to lysosomal proteases), from different types of lipid vesicles. We anticipate that measurement of ENM-induced movement of proteins across model lipid membranes may give further insight into the biological processes of LMP and the kinds of ENM that can produce it.
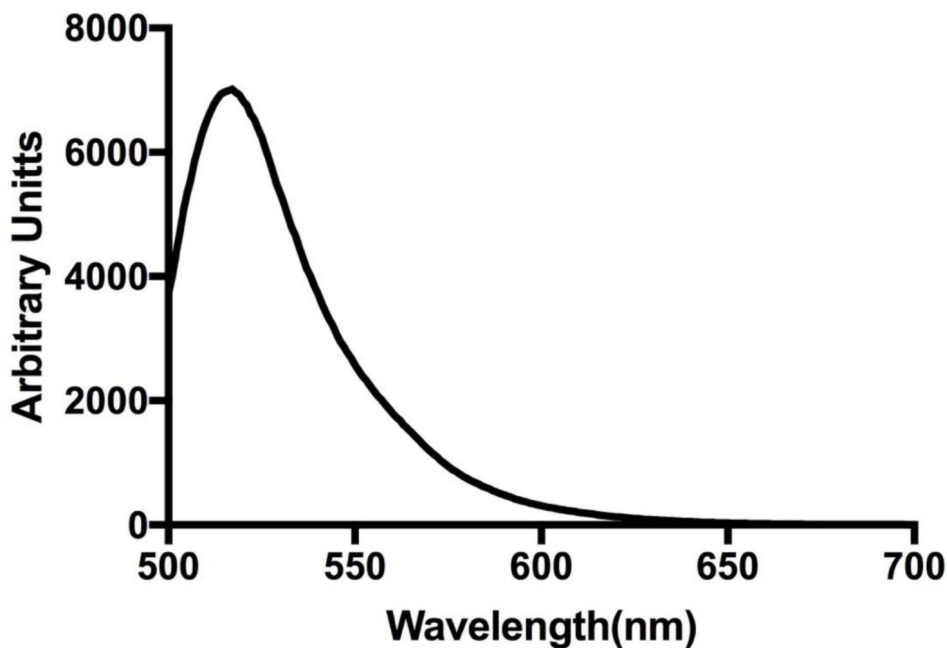
Acknowledgments

Appendix

Figure 1: Calcein Loaded Liposome Fluorescence Emission Spectrum
Liposomes loaded with 50 mM calcein were excited at 490 nm and an emission spectrum collected on a SpectraMax M4. The emission spectrum was measured at 1 nm increments.

Time-resolved Anisotropy Theory and Equations

$$r(t) = \frac{I_{VV}(t) - I_{VH}(t)}{I_{VV}(t) + 2I_{VH}(t)}$$

Equation#1

The anisotropy is given by the value, r. The total intensity is defined by the tern I(t), while the vertical and horizontal emission decays are I_{VV} and I_{VH}, respectively.

$$S^2 = \frac{r_\infty}{r_o} = \left[\frac{1}{2}\cos(\theta)(1 + \cos(\theta))\right]^2$$

Equation #2

The order parameter, S, represents the order of a lipid membrane and is defined by the relationship of r_∞/r_0. In a lipid membrane, the initial anisotropy is r_0, while the residual anisotropy that the fluorescence probe decays to is r_∞. This relationship between r_0 and r_∞ can be used to determine a range of motion of the fluorescence probe, or a wobble-in-a-cone angle, θ.

$$\% \text{ Leakage} = [(I_t - I_0)/(I_{max} - I_0)] * 100$$

Equation #3

The percent of calcein leakage was calculated by subtracting the background intensity, I_0, from the intensity after incubation (I_t) and the total intensity (I_{max}) upon complete lysis. Then I_t is divided by I_{max} and multiplied by 100 to generate a percentage.
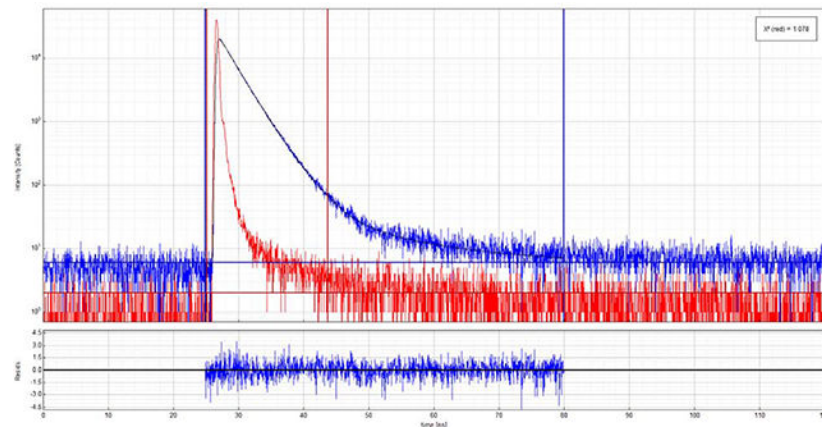
Example of Anisotropy Decay Curves

VV
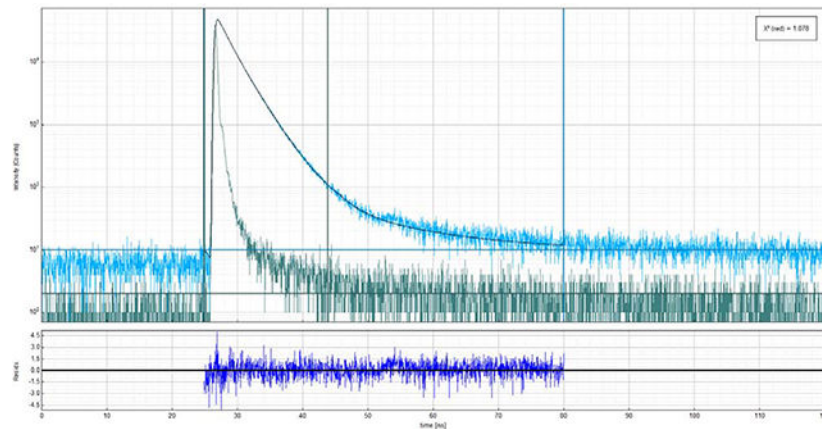
Above is an example anisotropy decay for vertically (90°) polarized excitation with vertically polarized emission.

VH

Above is an example anisotropy decay for vertically (90°) polarized excitation with horizontally (0°) polarized emission.

Table 1:

Mean Cone Angle Values

Lipids	Treatment		
	Control	**TiO$_2$**	**ZnO**
DOPC	35.9 ± 1.6	36.2 ± 0.4	36.6 ± 4.9
DOPC-chol	20.6 ± 1.2	15.9 ± 1.5	18.5 ± 0.8
DOPS	35.4 ± 1.4	32.9± 0.5	25.5 ± 2.3
DOPS-chol	20.6 ± 1.2	18.9 ± 1.5	17.9 ± 0.5

Lipids	Treatment		
	Control	TiO$_2$	ZnO
POPC	33.9 ± 1.6	27.9 ± 3.3	33.8 ± 2.1
POPC-chol	16.7 ± 2.9	13.9 ± 3.9	15.9 ± 3.4

Listed in the table are mean cone angle values for triplicate experiments with the standard deviation shown.

References

(1). Vance ME; Kuiken T; Vejerano EP; McGinnis SP; Hochella MF; Rejeski D; Hull MS Nanotechnology in the Real World: Redeveloping the Nanomaterial Consumer Products Inventory. Beilstein J. Nanotechnol. 2015, 6, 1769–1780. 10.3762/bjnano.6.181. [PubMed: 26425429]

(2). Borm PJ; Robbins D; Haubold S; Kuhlbusch T; Fissan H; Donaldson K; Schins R; Stone V; Kreyling W; Lademann J The Potential Risks of Nanomaterials: A Review Carried out for ECETOC. Particle and fibre toxicology 2006, 3 (1), 11. [PubMed: 16907977]

(3). Sahu SC; Hayes AW Toxicity of Nanomaterials Found in Human Environment: A Literature Review. Toxicology Research and Application 2017, 1, 239784731772635 10.1177/2397847317726352.

(4). Hamilton RF; Wu N; Porter D; Buford M; Wolfarth M; Holian A Particle Length-Dependent Titanium Dioxide Nanomaterials Toxicity and Bioactivity. Part. Fibre Toxicol. 2009, 6 (1), 35 10.1186/1743-8977-6-35. [PubMed: 20043844]

(5). Hamilton RF; Wu Z; Mitra S; Shaw PK; Holian A Effect of MWCNT Size, Carboxylation, and Purification on in Vitro and in Vivo Toxicity, Inflammation and Lung Pathology. Part. Fibre Toxicol 2013, 10 (1), 57. [PubMed: 24225053]

(6). Hamilton RF; Wu N; Xiang C; Li M; Yang F; Wolfarth M; Porter DW; Holian A Synthesis, Characterization, and Bioactivity of Carboxylic Acid-Functionalized Titanium Dioxide Nanobelts. Part. Fibre Toxicol. 2014, 11 (1), 43. [PubMed: 25179214]

(7). Hussain S; Thomassen LCJ; Ferecatu I; Borot M-C; Andreau K; Martens JA; Fleury J; Baeza-Squiban A; Marano F; Boland S Carbon Black and Titanium Dioxide Nanoparticles Elicit Distinct Apoptotic Pathways in Bronchial Epithelial Cells. Part. Fibre Toxicol. 2010, 7, 10–10. 10.1186/1743-8977-7-10. [PubMed: 20398356]

(8). Jessop F; Hamilton RF; Rhoderick JF; Fletcher P; Holian A Phagolysosome Acidification Is Required for Silica and Engineered Nanoparticle-Induced Lysosome Membrane Permeabilization and Resultant NLRP3 Inflammasome Activity. Toxicol. Appl. Pharmacol. 2017, 318, 58–68. 10.1016/j.taap.2017.01.012. [PubMed: 28126413]

(9). Sohaebuddin SK; Thevenot PT; Baker D; Eaton JW; Tang L Nanomaterial Cytotoxicity Is Composition, Size, and Cell Type Dependent. Part. Fibre Toxicol. 2010, 7, 22–22. 10.1186/1743-8977-7-22. [PubMed: 20727197]

(10). Johansson A-C; Appelqvist H; Nilsson C; Kågedal K; Roberg K; Öllinger K Regulation of Apoptosis-Associated Lysosomal Membrane Permeabilization. Apoptosis 2010, 15 (5), 527–540. 10.1007/s10495-009-0452-5. [PubMed: 20077016]

(11). Zhou R; Yazdi AS; Menu P; Tschopp J A Role for Mitochondria in NLRP3 Inflammasome Activation. Nature 2011, 469 (7329), 221–225. 10.1038/nature09663. [PubMed: 21124315]

(12). Fantuzzi G; Dinarello CA Interleukin-18 and Interleukin-1β: Two Cytokine Substrates for ICE (Caspase-1). Journal of Clinical Immunology 1999, 19 (1), 1–11. 10.1023/A:1020506300324. [PubMed: 10080100]

(13). Martinon F; Burns K; Tschopp J The Inflammasome: A Molecular Platform Triggering Activation of Inflammatory Caspases and Processing of proIL-β. Mol. Cell 2002, 10 (2), 417–426. 10.1016/S1097-2765(02)00599-3. [PubMed: 12191486]

(14). Wang L; Manji GA; Grenier JM; Al-Garawi A; Merriam S; Lora JM; Geddes BJ; Briskin M; DiStefano PS; Bertin J PYPAF7, a Novel PYRIN-Containing Apaf1-like Protein That Regulates

Activation of NF-κB and Caspase-1-Dependent Cytokine Processing. J. Biol. Chem. 2002, 277 (33), 29874–29880. 10.1074/jbc.M203915200. [PubMed: 12019269]

(15). Dinarello C Biologic Basis for Interleukin-1 in Disease. Blood 1996, 87 (6), 2095. [PubMed: 8630372]

(16). Dinarello CA Immunological and Inflammatory Functions of the Interleukin-1 Family. Annual Review of Immunology 2009, 27 (1), 519–550. 10.1146/annurev.immunol.021908.132612.

(17). Lamkanfi M; Dixit VM Inflammasomes and Their Roles in Health and Disease. Annual Review of Cell and Developmental Biology 2012, 28 (1), 137–161. 10.1146/annurev-cellbio-101011-155745.

(18). Biological Effects of Fibrous and Particulate Substances; Otsuki T, Yoshioka Y, Holian A, Eds.; Current Topics in Environmental Health and Preventive Medicine; Springer Japan: Tokyo, 2016.

(19). Appelqvist H; Nilsson C; Garner B; Brown AJ; Kågedal K; Öllinger K Attenuation of the Lysosomal Death Pathway by Lysosomal Cholesterol Accumulation. The American Journal of Pathology 2011, 178 (2), 629–639. 10.1016/j.ajpath.2010.10.030. [PubMed: 21281795]

(20). Appelqvist H; Sandin L; Björnström K; Saftig P; Garner B; Öllinger K; Kågedal K Sensitivity to Lysosome-Dependent Cell Death Is Directly Regulated by Lysosomal Cholesterol Content. PLoS ONE 2012, 7 (11), e50262 10.1371/journal.pone.0050262. [PubMed: 23166840]

(21). Holmberg JP; Ahlberg E; Bergenholtz J; Hassellöv M; Abbas Z Surface Charge and Interfacial Potential of Titanium Dioxide Nanoparticles: Experimental and Theoretical Investigations. Journal of Colloid and Interface Science 2013, 407, 168–176. 10.1016/j.jcis.2013.06.015. [PubMed: 23859811]

(22). An SSA; Kim K; Choi M; Lee J-K; Jeong J; Kim Y-R; Kim M-K; Paek S; Shin J-H Physicochemical Properties of Surface Charge-Modified ZnO Nanoparticles with Different Particle Sizes. International Journal of Nanomedicine 2014, 41 10.2147/IJN.S57923. [PubMed: 25565825]

(23). Xia T; Hamilton RF; Bonner JC; Crandall ED; Elder A; Fazlollahi F; Girtsman TA; Kim K; Mitra S; Ntim SA; et al. Interlaboratory Evaluation of *in Vitro* Cytotoxicity and Inflammatory Responses to Engineered Nanomaterials: The NIEHS Nano GO Consortium. Environmental Health Perspectives 2013, 121 (6), 683–690. 10.1289/ehp.1306561. [PubMed: 23649538]

(24). Owen DM; Lanigan PMP; Dunsby C; Munro I; Grant D; Neil MAA; French PMW; Magee AI Fluorescence Lifetime Imaging Provides Enhanced Contrast When Imaging the Phase-Sensitive Dye Di-4-ANEPPDHQ in Model Membranes and Live Cells. Biophys. J. 2006, 90 (11), L80–L82. 10.1529/biophysj.106.084673. [PubMed: 16617080]

(25). Obaid AL; Loew LM; Wuskell JP; Salzberg BM Novel Naphthylstyryl-Pyridinium Potentiometric Dyes Offer Advantages for Neural Network Analysis. J. Neurosci. Methods 2004, 134 (2), 179–190. 10.1016/j.jneumeth.2003.11.011. [PubMed: 15003384]

(26). Minazzo AS; Darlington RC; Ross JBA Loop Dynamics of the Extracellular Domain of Human Tissue Factor and Activation of Factor VIIa. Biophysical Journal 2009, 96 (2), 681–692. 10.1016/j.bpj.2008.10.018. [PubMed: 19167313]

(27). Alkhammash HI; Li N; Berthier R; de Planque MRR Native Silica Nanoparticles Are Powerful Membrane Disruptors. Physical Chemistry Chemical Physics 2015, 17 (24), 15547–15560. 10.1039/C4CP05882H. [PubMed: 25623776]

(28). Jin L; Millard AC; Wuskell JP; Clark HA; Loew LM Cholesterol-Enriched Lipid Domains Can Be Visualized by Di-4-ANEPPDHQ with Linear and Nonlinear Optics. Biophys. J. 2005, 89 (1), L04–L06. 10.1529/biophysj.105.064816. [PubMed: 15879475]

(29). Kilin V; Glushonkov O; Herdly L; Klymchenko A; Richert L; Mely Y Fluorescence Lifetime Imaging of Membrane Lipid Order with a Ratiometric Fluorescent Probe. Biophys. J. 2015, 108 (10), 2521–2531. 10.1016/j.bpj.2015.04.003. [PubMed: 25992730]

(30). Steele HBB; Sydor MJ; Anderson DS; Holian A; Ross JBA Using Time-Resolved Fluorescence Anisotropy of Di-4-ANEPPDHQ and F2N12S to Analyze Lipid Packing Dynamics in Model Systems. Journal of Fluorescence 2019, 29 (2), 347–352. 10.1007/s10895-019-02363-7. [PubMed: 30937610]

(31). Lakowicz JR Principles of Fluorescence Spectroscopy, 3rd ed.; Springer: New York, 2006.

(32). Kinosita K; Ikegami A; Kawato S On the Wobbling-in-Cone Analysis of Fluorescence Anisotropy Decay. Biophysical Journal 1982, 37 (2), 461–464. 10.1016/S0006-3495(82)84692-4. [PubMed: 7059650]

(33). van Meer G; de Kroon AIPM Lipid Map of the Mammalian Cell. Journal of Cell Science 2011, 124 (1), 5–8. 10.1242/jcs.071233. [PubMed: 21172818]

(34). Róg T; Pasenkiewicz-Gierula M; Vattulainen I; Karttunen M Ordering Effects of Cholesterol and Its Analogues. Biochimica et Biophysica Acta (BBA) - Biomembranes 2009, 1788 (1), 97–121. 10.1016/j.bbamem.2008.08.022. [PubMed: 18823938]

(35). Ipsen JH; Karlström G; Mourtisen OG; Wennerström H; Zuckermann MJ Phase Equilibria in the Phosphatidylcholine-Cholesterol System. Biochim. Biophys. Acta BBA-Biomembr. 1987, 905 (1), 162–172.

(36). Dufourc EJ; Parish EJ; Chitrakorn S; Smith ICP Structural and Dynamical Details of Cholesterol-Lipid Interaction as Revealed by Deuterium NMR. Biochemistry 1984, 23 (25), 6062–6071. 10.1021/bi00320a025.

(37). Owen JS; Bruckdorfer KR; Day RC; McIntyre N Decreased Erythrocyte Membrane Fluidity and Altered Lipid Composition in Human Liver Disease. Journal of Lipid Research 1982, 23 (1), 124–132. [PubMed: 7057101]

(38). Turci F; Pavan C; Leinardi R; Tomatis M; Pastero L; Garry D; Anguissola S; Lison D; Fubini B Revisiting the Paradigm of Silica Pathogenicity with Synthetic Quartz Crystals: The Role of Crystallinity and Surface Disorder. Particle and Fibre Toxicology 2015, 13 (1). 10.1186/s12989-016-0136-6.

(39). Ziglari T; Anderson DS; Holian A Determination of the Relative Contribution of the Non-Dissolved Fraction of ZnO NP on Membrane Permeability and Cytotoxicity.Inhalation Toxicology 2020, 32 (2), 86–95. 10.1080/08958378.2020.1743394. [PubMed: 32216500]

(40). Zhang J; Qin X; Wang B; Xu G; Qin Z; Wang J; Wu L; Ju X; Bose DD; Qiu F; Zhou H; Zou Z Zinc Oxide Nanoparticles Harness Autophagy to Induce Cell Death in Lung Epithelial Cells. Cell Death & Disease 2017, 8 (7), e2954–e2954. 10.1038/cddis.2017.337. [PubMed: 28749469]

(41). Lin J; Alexander-Katz A Cell Membranes Open "Doors" for Cationic Nanoparticles/Biomolecules: Insights into Uptake Kinetics. ACS Nano 2013, 7 (12), 10799–10808. 10.1021/nn4040553. [PubMed: 24251827]

(42). Ding H; Ma Y Computer Simulation of the Role of Protein Corona in Cellular Delivery of Nanoparticles. Biomaterials 2014, 35 (30), 8703–8710. 10.1016/j.biomaterials.2014.06.033. [PubMed: 25005681]

(43). Taylor U; Klein S; Petersen S; Kues W; Barcikowski S; Rath D Nonendosomal Cellular Uptake of Ligand-Free, Positively Charged Gold Nanoparticles. Cytometry Part A 2010, 9999A, NA–NA. 10.1002/cyto.a.20846.

(44). Verma A; Uzun O; Hu Y; Hu Y; Han H-S; Watson N; Chen S; Irvine DJ; Stellacci F Surface-Structure-Regulated Cell-Membrane Penetration by Monolayer-Protected Nanoparticles. Nature Materials 2008, 7 (7), 588–595. 10.1038/nmat2202. [PubMed: 18500347]

(45). Zanella D; Bossi E; Gornati R; Faria N; Powell J; Bernardini G The Direct Permeation of Nanoparticles through the Plasma Membrane Transiently Modifies Its Properties. Biochimica et Biophysica Acta (BBA) - Biomembranes 2019, 1861 (10), 182997 10.1016/j.bbamem.2019.05.019. [PubMed: 31150635]

(46). Wang X; Li X; Wang H; Zhang X; Zhang L; Wang F; Liu J Charge and Coordination Directed Liposome Fusion onto SiO 2 and TiO 2 Nanoparticles. Langmuir 2019, 35 (5), 1672–1681. 10.1021/acs.langmuir.8b02979. [PubMed: 30558422]

(47). Liu Y; Liu J Leakage and Rupture of Lipid Membranes by Charged Polymers and Nanoparticles. Langmuir 2020, 36 (3), 810–818. 10.1021/acs.langmuir.9b03301. [PubMed: 31910024]

Highlights

- Engineered Nano-materials change lipid order in model systems

- Engineered Nano-materials cause membrane permeability to calcein

- Addition of cholesterol to lipid model systems changed lipid order
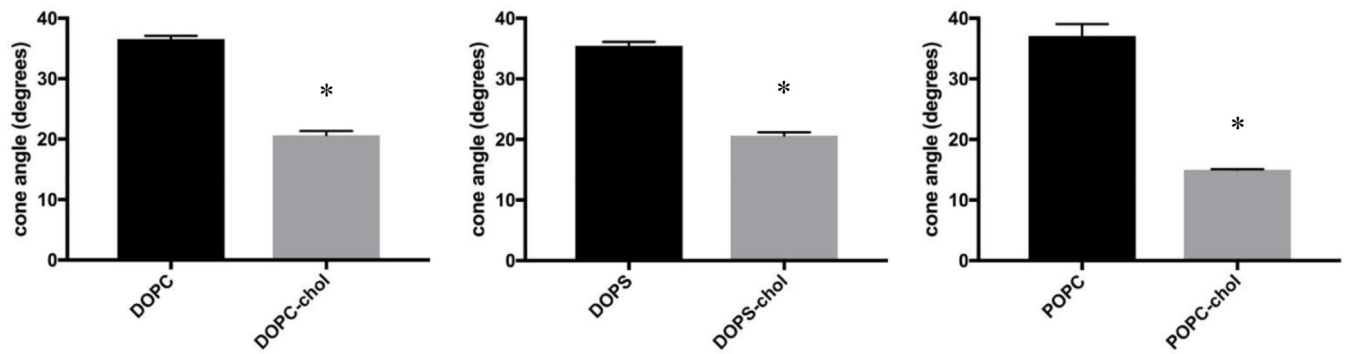
Figure 1:
Time-resolved Anisotropy of Model Liposomes with and without Cholesterol. Anisotropy data is displayed in degrees of the wobble-in-a-cone angle. Unpaired t-tests were used to compare untreated liposomes to ENM treated. * indicates p<0.05. n=3–5
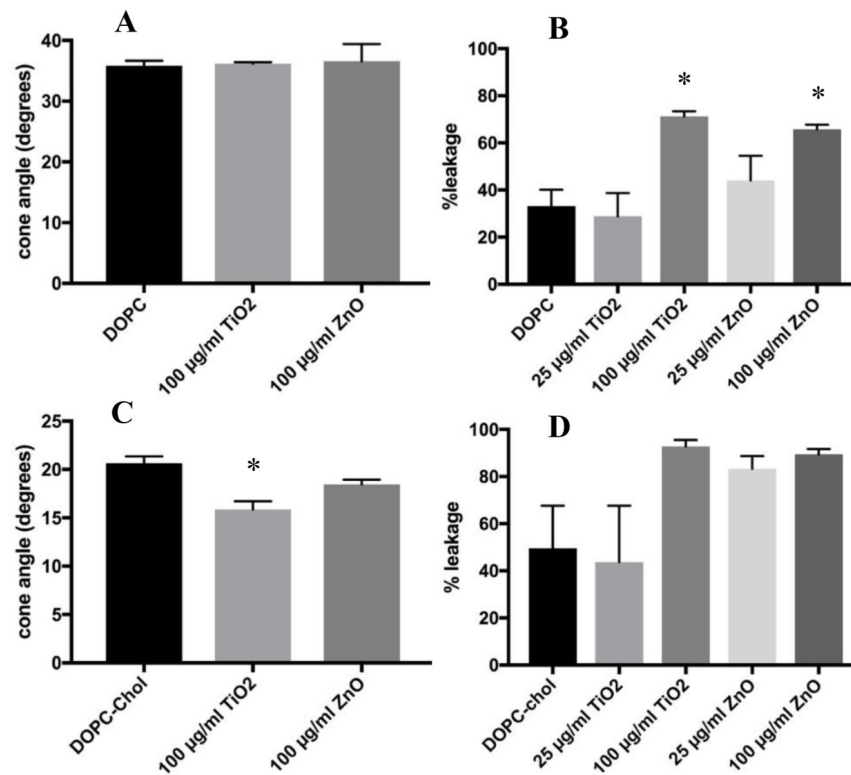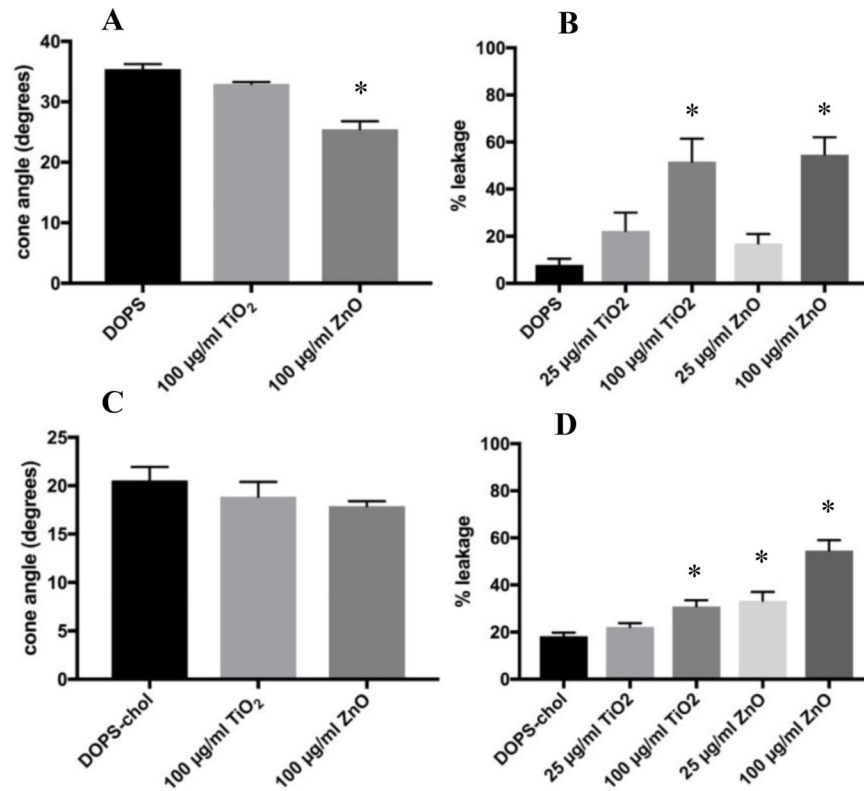
Figure 2:
Time-resolved Anisotropy and Calcein Leakage of DOPC Liposomes Treated with ENM. The doses of ENM was 100 μg/ml for 2 hours. Anisotropy data is displayed in degrees of the wobble-in-a-cone angle. Calcein leakage for ENM exposures were at 25 and 100 μg/ml after 2 hours. Percent leakage was calculated by using equation #3. Unpaired One-way ANOVA with Dunnett post-test were used to compare untreated liposomes to ENM treated. * indicates $p < 0.05$. n=3

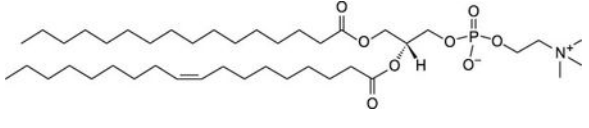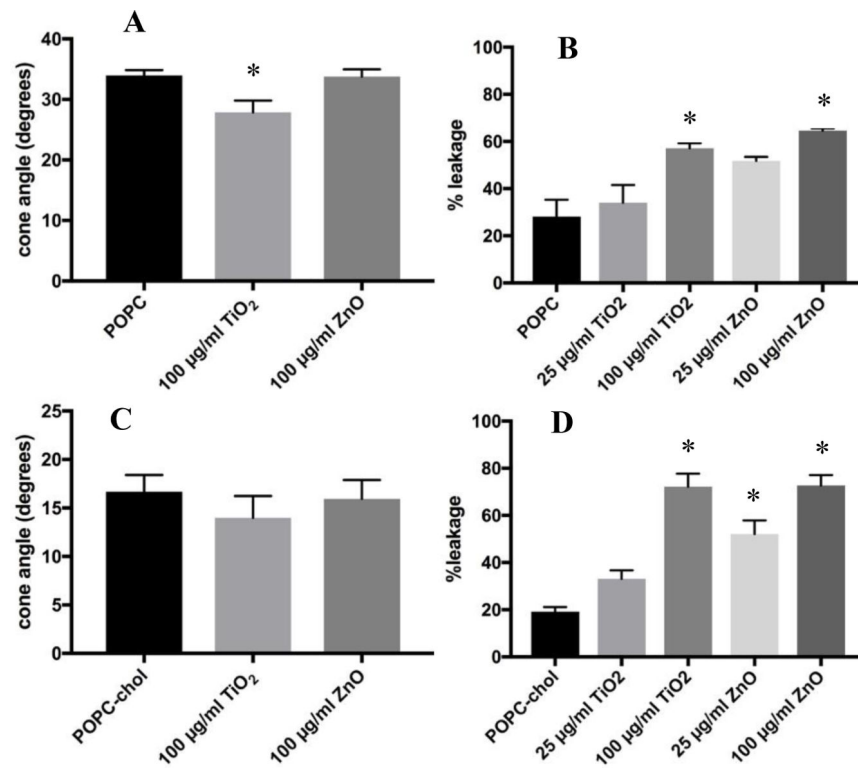**Figure 3:**
Time-resolved Anisotropy and Calcein Leakage of DOPS Liposomes Treated with ENM. The doses of ENM was 100 μg/ml for 2 hours. Anisotropy data is displayed in degrees of the wobble-in-a-cone angle. Calcein leakage for ENM exposures were at 25 and 100 μg/ml after 2 hours. Percent leakage was calculated by using equation #3. Unpaired One-way ANOVA with Dunnett post-test were used to compare untreated liposomes to ENM treated. * indicates $p < 0.05$. n=3
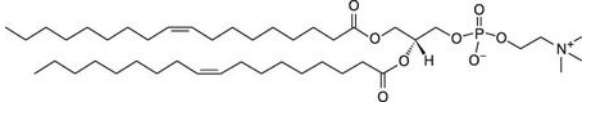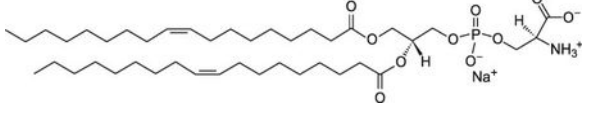
Figure 4:
Time-resolved Anisotropy and Calcein Leakage of POPC Liposomes Treated with ENM. The doses of ENM was 100 μg/ml for 2 hours. Anisotropy data is displayed in degrees of the wobble-in-a-cone angle. Calcein leakage for ENM exposures were at 25 and 100 μg/ml after 2 hours. Percent leakage was calculated by using equation #3. Unpaired One-way ANOVA with Dunnett post-test were used to compare untreated liposomes to ENM treated. * indicates $p < 0.05$. n=3

Table 1.

Phospholipids Used for Model Liposomes.

Lipid	Structure	Overall Charge	Phase Transition Temperature (°C)
POPC		Neutral	−2
DOPC		Neutral	−17
DOPS		−1	−11